https://doi.org/10.37982/hmc.57.1.4

Professional paper
Stručni rad

PROJECTING THE IMPACT OF CLIMATE CHANGE ON PRECIPITATION AMOUNT DISTRIBUTION AND SCENARIO IN THE AWASH RIVER BASIN (ETHIOPIA) THROUGH GCM DOWNSCALING

Projekcije utjecaja klimatskih promjena na razdiobu količine oborine i scenarij za sliv rijeke Awash (Etiopija) primjenom metode prilagodbe globalnog klimatskog modela

ABRHAME WELDEYOHANNES GILGEL[1,2]
TESEMASH ABEBE[1]

[1]Ethiopian Forestry Development, P.O.BOX 24536 code 1000, Addis Ababa, Ethiopia
[2]Ethiopian Meteorology Institute, P.O.BOX 1090, Addis Ababa, Ethiopia

abrhame.gilgel@gmail.com

Received 27 February 2024, in final form 31 January 2025
Primljeno 27. veljače 2024., u konačnom obliku 31. siječnja 2025.

Abstract: The objective of this research is to develop climate change scenario for precipitation case over Awash River Basin in Ethiopia under three representative concentration pathways (RCPs) of greenhouse gases in atmosphere which stabilising radiative forcing scenarios at 2.6, 4.5 and 8.5 Wm^{-2} until year 2100, indicated as RCP2.6, RCP4.5 and RCP8.5, respectively. The method used to generate climate change scenarios for each RCPs is Statistical Downscaling Method (SDSM) of climate scenarios from global to regional scale. For performance of SDSM model calibration and evaluation Nash-Sutcliffe efficiency (NSE) and determination coefficients (R^2) are used. The results in this study showed that the SDSM model demonstrated moderate to very good strength ($R^2 \geq 0.7$; NSE ≥ 0.7) for calibration and validation coefficient values on average, respectively. Concerning climate change scenario projections, future changes are expected to be slight or moderate until the 2020s. However, after this period, the model predict an increase in annual precipitation amount, especially in the medium and high emission scenarios (RCP4.5 and RCP8.5). Significant change is observed in the periods 2050s and 2080s under each RCP. Regarding monthly precipitation performance the model exhibited an increase rainfall ranging from +1% up to +85%, but on some months a decrease is observed ranging from -1% up to -40%, compared to the baseline period (1983–2016). On seasonal basis, in Upper and Middle Awash River Basin the highest change in precipitation amount increment is expected to be in the Belg season (spring). When we consider the future annual precipitation amount, the Lower Awash River Basin is expected to experience the highest increase changes in precipitation amount among all three sub-basins.
In general, we conclude that the future precipitation amount will significantly increase in time over the Awash River Basin. As a result, the Awash River Basin will be vulnerable to flooding due to the anticipated increase in precipitation brought on by global climate change; and are likely to have moderate to significant negative impacts on various socioeconomic activities over the communities and natural resources existing over Awash River Basin. Therefore,

we recommend that in order to create better climate change adaptation and mitigation mechanisms, decision-makers are provided with this information and consider with other related findings to strengthen the national adaptation and mitigation strategies.

Key words: downscaling climate models, climate change scenarios, precipitation amount distribution, environmental impacts

Sažetak: Cilj je ovog rada izraditi scenarij klimatskih promjena za količinu oborine u slivu rijeke Awash u Etiopiji za tri slučaja koncentracija stakleničkih plinova u atmosferi (engl. *Representative Concentration Pathways – RCPs*) odnosno radijacijsko forsiranje na 2,6, 4,5 i 8,5 Wm^{-2} do 2100. godine, označeni kao RCP2,6, RCP4,5 i RCP8,5. Za generiranje scenarija klimatskih promjena za svaki RCP primijenjena je metoda statističke prilagodbe s globalne na regionalnu skalu (engl. *Statistical Downscaling Method – SDSM*). Za ocjenu karakteristika SDSM modela korišteni su Nash-Sutcliffe efikasnost (NSE) i koeficijent determinacije (R^2). Prema rezultatima ove studije SDSM model pokazuje umjerenu do vrlo dobru pouzdanost ($R^2 \geq 0{,}7$; NSE $\geq 0{,}7$) za prosječne vrijednosti koeficijenata kalibracije i validacije. Kad je riječ o projekcijama scenarija klimatskih promjena, očekuje se da će promjene biti minimalne ili umjerene do 2020-ih u slučaju godišnjih količina oborine. Međutim, nakon tog razdoblja model predviđa povećanje godišnje količine oborine, posebno za srednji i nepoželjan scenarij (RCP4,5 i RCP8,5). Značajna promjena uočena je u razdobljima 2050-ih i 2080-ih za svaki RCP. Za mjesečne količine oborine model pokazuje povećanje od +1 % do +85 %, ali za neke mjesece i smanjenje količine oborine od -1 % do -40 % u odnosu na referentno razdoblje 1983. – 2016. Gledajući po sezonama, u gornjem i srednjem slivu rijeke Awash očekuje se najveće povećanje količine oborine u sezoni Belg (veljača – svibanj). Model predviđa najveći porast srednje godišnje količine oborine u donjem slivu rijeke Awash.
Može se zaključiti da će klimatske promjene utjecati na značajno povećanje količine oborine s vremenom u slivu rijeke Awash povećavajući rizik od poplava što će vjerojatno imati umjereni do značajan negativni utjecaj na različite socioekonomske aktivnosti zajednice i prirodne resurse.
Stoga preporučujemo da se o ovome informiraju donositelji odluka kako bi se stvorili bolji mehanizmi za prilagodbu klimatskim promjenama i njihovo ublažavanje te da se uz druge odredbe razmotri jačanje nacionalnih strategija za prilagodbu i ublažavanje posljedica klimatskih promjena.

Ključne riječi: downscaling klimatskih modela, scenariji klimatskih promjena, razdioba oborine i utjecaji na okoliš

1. INTRODUCTION

One of the biggest issues facing the globe now is climate change. It is expected to accelerate in all regions in the coming decades, with increased heat waves, longer warm seasons, and shorter cold seasons (IPCC, 2014, 2021). Global warming of 1.5 to 2.0°C will be exceeded during the 21st century unless deep reductions in CO_2 and other greenhouse gas emissions occur in the coming decades (IPCC, 2014, 2021). Rainfall patterns are being influenced by climate change (IPCC, 2014, 2021; Ranasinghe et al., 2021). At the global scale, extreme daily precipitation events are projected to intensify by about 7% for each 1.0°C of global warming. Precipitation amount is expected to increase in high latitudes, whereas it is expected to decrease in the subtropics. Monsoon precipitation is likely to change, with regional variations (IPCC, 2021; McCarthy et al., 2001; Frich et al., 2002).

East Africa is anticipated to experience higher temperatures, strong precipitation variability, and intense wet spells leading to widespread pluvial flooding events hitting most countries including Ethiopia, Somalia, Kenya, and Tanzania (Gebrechorkos, Huelsmann and Bernhofer, 2019; Haile et al., 2020). Increased temperatures are also projected to result in more intense heat waves and increased evapotranspiration rates, which will have an impact on a variety of factors of local economic growth and agricultural output. Temperature rise, as well as an increase in the frequency and intensity of major droughts and floods, will certainly lower crop yields and cause animal losses, posing a serious threat to food security (IPCC, 2021; Houghton et al., 2001; Ranasinghe et al., 2021).

Increased temperatures are predicted for East Africa, especially for Ethiopia, under a high-emission scenario, with mean monthly temperature variations predicted to increase by 1.8°C by the 2050s and by 3.7°C by the end of the century (Gebrechorkos, Huelsmann and Bernhofer, 2019; IPCC, 2021). Ethiopia has a high level of inter-annual variability, and there is still a lot of uncertainty around its precipitation trends in the future. The spring and summer rainfall in the southern and central regions could decrease by as much as 20%, according to projected patterns. While an overall decrease in rainfall is anticipated for northern areas, an increase is anticipated for the southwest and southeast (Gebrechorkos, Huelsmann and Bernhofer, 2018; NAPA-ETH, 2019). The entire nation's projected warming trends are predicted to exacerbate the already observed drop in rainfall, increasing water stress. Higher temperatures will speed up evapotranspiration, diminishing the benefits of increased rainfall, while precipitation amount is predicted to increase in some parts of East Africa, placing additional strain on water resources (Berhanu and Beyene, 2015; IPCC, 2021; Houghton et al., 2001).

Global climate models (GCMs) have taken over as the main tool for acquiring information about the climate on a range of spatial and temporal dimensions as a result of advances in our knowledge of the physical processes that underlie climate systems (Eden and Widmann, 2014; Mishra et al., 2014; Hutchinson et al., 2009). However, GCMs have limited capacity to capture sub grid-scale features, and outputs from GCMs are still subject to biases (Hui et al., 2019; Dibike and Coulibaly, 2005). They also have a finite capacity for studying hydrological processes and physical atmospheric processes at the regional scale (Lee, Camargo, Sobel and Tippet, 2020; Dirmeyer, Jin and Yan, 2013; Zhao, Xu, Huang and Li, 2008). Regional climate change has attracted considerable attention because of the rising economic losses from weather and climate-related disasters (Fan, Jiang and Gou, 2021; Fowler, Blenkinsop and Tebaldi, 2007; Yang et al., 2020).

In the last 20 years, a variety of statistical downscaling methods (SDSM) have been developed with a broad range of application in regional climate change (Tavakol-Davani, Nasseri and Zahraie, 2013; Behera et al., 2016). SDSM is a typical statistical downscaling tool that combines regression methods and a weather generator (Wilby et al., 2000; Fenglin et al., 2023), and it has been widely applied in many fields. According to prior studies, SDSM is an acceptable and trustworthy downscaling method that performs well in downscaling air surface temperature, evaporation, and precipitation amount. It has been used to project future climate changes in many regions (Poitras et al., 2011; Hassan, Shamsudin and Harun, 2013; Liu, Kummerow and Elsaesser, 2017). To analyse the future climatic scenario, the current study uses statistical downscaling model (SDSM) methods (Wilby et al., 2014; Behera et al., 2016) that use the multiple linear regression approach to downscale GCM outputs from global scale to local scale. Therefore, the main purpose of this study is to statistically downscale and generate climate scenarios for future precipitation amount of the study area under low (RCP2.6), medium (RCP4.5) and high (RCP8.5) representative concentration pathways for the periods 2020's, 2050's and 2080's.

2. METHODS

2.1. Description of study area

Awash River Basin is one of the nine basins in Ethiopia; and it is unique from the others in that it does not have cross boundary flow. The geographic location of the Awash River Basin is between 7°53'N and 12°N of latitudes and 37°57'E and 43°25'E of longitudes. The largest part of the Awash River Basin is located in the arid lowlands of the Afar Region in the northeastern part of Ethiopia

(Fig. 1). The total length of the main course is about 1200 km, and it is the principal stream of an endorheic drainage basin covering parts of the Oromia, Somali, Amhara, and Afar region (Koriche, Rientjes, Haile and Bekele, 2012). The Awash River Basin is the most important basin in Ethiopia and covers a total land area of 110 000 km^2 and serves as home to 10.5 million inhabitants (Fenglin et al., 2023; Abayneh, Ephrem and Hayal, 2024). The river rises on the high plateau near Ginchi town, in the west side of the capital city of Addis Ababa, Ethiopia and flows along the Rift Valley into the Afar Triangle and terminates in the salty Lake Abbe on the border with Djibouti (Fenglin et al., 2023; Abayneh, Ephrem and Hayal, 2024).

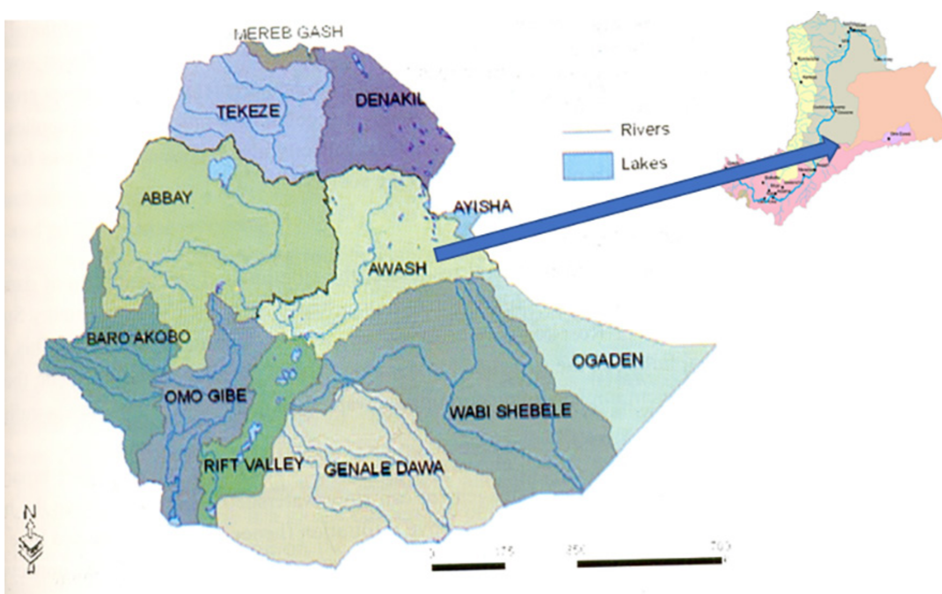

Figure 1. Map of study area: Awash River Basin Catchment area (source: Awash River Basin Authority, 2014).

Slika 1. Karta istraživanog područja: područje sliva rijeke Awash (izvor: Awash River Basin Authority, 2014).

Climate of Awash River Basin: The river basin extends from semi-desert lowlands to cold high mountainous zones with extreme ranges of temperature and rainfall (Romilly and Gebremichael, 2010). There are three seasons in the Awash River Basin based on the movement of the Inter-Tropical Convergence Zone (ITCZ), the amount of rainfall and the rainfall timing. The three seasons are Kiremt, which is the main rainy season (June–September), Bega, which is the dry season (October–January), and Belg, the small rainy season (February–May), (Gilgel, Terefe and Asfaw, 2019; Degefu, 1987). The mean annual rainfall amount varies from 1600 mm in the elevated areas to 160 mm in the Lower Awash River Basin. In the same way, the mean annual temperature of Awash River Basin ranges from 20.8°C in the upper part to 29.0°C in the lower part.

2.2. Methodology

2.2.1. Details of methods

In statistical downscaling method (SDSM) (Fig. 2), the first step before model calibration is quality control using SDSM through identification of gross data errors, missing data codes and outliers to get the appropriate quality data. The screening predictor variables are done by trial-and-error procedure for model calibration. Using the partial correlations statistics, predictors which showed the strongest association with the predictand are selected. Assembly and calibration of statistical downscaling model(s) the large-scale predictor variables identified are used in the determination of multiple linear regression relationships between these variables and the local station data. Then, the

SDSM manual procedure is followed to generate a climate scenario for the basins. Data sources observed daily precipitation amount data and are obtained from weather stations located in or near the watershed. GCM-derived predictors are generated from a global database. Screening of the potential predictors for the selected predictand (i.e. observed precipitation) is used to select the appropriate downscaling predictors for model calibration and the most crucial and decisive part in statistical downscaling model. This is done by identifying an appropriate large-scale gridded predictor's result in good correlation between observed and downscaled climate variables during model calibration and scenario generation. The recommended method for screening the potential predictors is starting the processes by selecting seven or eight predictors at a time and analyse their explained variance, then select those predictors which has higher explained variance (the significance level which tests the significance of predictor-predictand correlation was set to the default P<0.05) and drop the rest.

For the selected predictor their correlation matrix is analysed or calculated with the observed predictand. This procedure is repeated by holding those predictors which pass the above criteria and add new predictors from the reset of available predictors. Model calibration is done for the period 1983–2000, and model validation is done for the period 2001–2016. The calibrated model is used to generate future scenarios using the CanESM2 predictors available under RCP2.6, RCP4.5, and RCP8.5.

So, in general, regarding climate change scenario projection, in this paper all these steps are carried out in the same procedure and design similar to Molla (2016; 2020), Feyissa, Zeleke, Bewket and Gebremariam (2018) and Wilby and Dawson (2007).

SDSM Description: The statistical downscaling method (SDSM) software reduces the task of statistically downscaling daily weather series into seven discrete steps: quality control and data transformation; screening of predictor variables; model calibration; weather generation; statistical analyses; scenario generation (Wilby and Dawson, 2007; Molla, 2020; Wilby et al., 2002; Huang et al., 2010; Zhao, Xu, Huang and Li, 2008). The future projection is based on CanESM2 predictors and different representative concentration pathways (RCP) (Giorgetta et al., 2013). The fifth assessment report used a new set of scenarios known as representative concentration pathways (RCPs) based on a set of anthropogenic forcing scenarios used for the new climate model simulations conducted within the framework of the CMIP5 (Van Vuuren et al., 2011; Arora and Boer, 2014; Separovic et al., 2013). Integrated assessment models (IAMs),

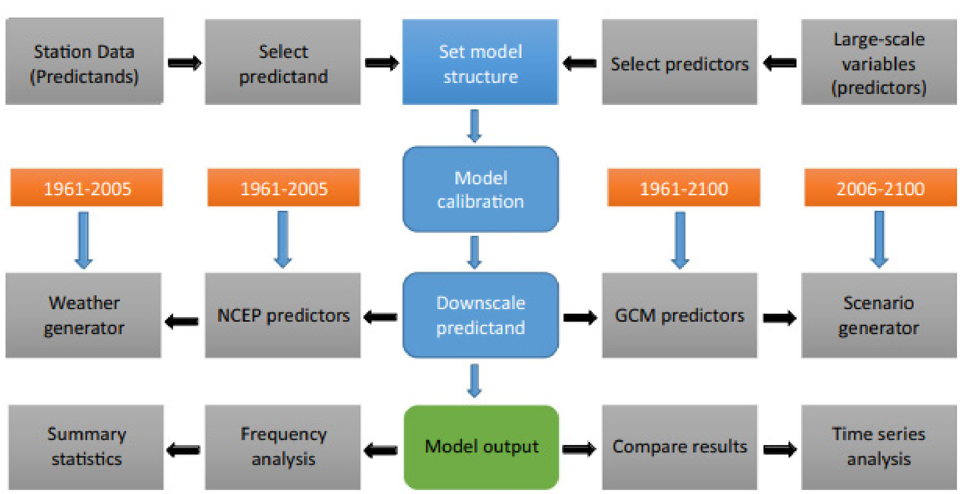

Figure 2. Schematic diagram of the statistical downscaling model (SDSM): adopted from Gebrechorkos, Huelsmann and Bernhofer (2019).

Slika 2. Shematski dijagram statističke prilagodbe modela (SDSM): preuzeto iz Gebrechorkos, Huelsmann i Bernhofer (2019).

which frequently contain economic, demographic, energy, and simple climatic components, have been used to construct RCPs. The RCPs should contain data of all radiative forcing elements (emissions of greenhouse gases, air pollutants, and land use) that are required as input for atmospheric chemistry modelling and climate modelling (Van Vuuren et al., 2011; Nakicenovic and Swart, 2000; Arora and Boer, 2014).

2.2.2. Data

We used daily precipitation amount station data to identify the most dominant predictors and develop the most accurate future climate scenarios. Observed daily precipitation data from 9 stations during the period 1983 to 2016 (baseline period) is collected from the National Meteorological Agency (NMA) of Ethiopia and 26 large scale climate variables (predictors) from the NCEP (National Centers for Environmental Prediction) (http://climate-scenarios.canada.ca/) reanalysis data and CanESM2 (second generation Canadian Earth System Model) are used for the downscaling process calibration, validation, and future projections.

For the whole Awash River catchment area, we use data from nine climate stations. Three of the climate stations are represented each sub-basin: Upper Awash, Middle Awash and Lower Awash River Basin. The coordinates and positions of the climate stations used under this study are presented as follows: Alem Tena (longitude: 38.90783, latitude: 8.29, altitude: 1654 meters above sea level (m.asl)), Guder (longitude: 39.75467, latitude: 8.95767, altitude: 2101 m.asl), Holeta (longitude: 38.49298, latitude: 9.0777, altitude: 2391 m.asl), Awash Arba (longitude: 40.15886, latitude: 9.141056, altitude: 986 m.asl), Shewa Robit (longitude: 39.89436, latitude: 10.0127, altitude: 1280 m.asl), Erer (longitude: 41.37922, latitude: 8.29, altitude: 1107 m.asl), Chefa (longitude: 39.81219, latitude: 10.84426, altitude: 1606 m.asl), Dire Dawa (longitude: 42.5333, latitude: 9.9667, altitude: 1180 m.asl) and Mille (longitude: 40.75, latitude: 11.416667, altitude: 496 m.asl).

2.2.3. Model performance evaluation

Regarding model performance evaluation, statistical regression models such as Nash-Sutcliffe Efficiency (NSE) and r-squared (R^2) are used. These statistics identify the amount of explanatory power of the predictor to explain the predictand and finally the scatter plot or bar graph is carried out in order to identify the nature of the correlation between observed and simulated:

$$R^2 = 1 - \frac{RSS}{TSS} = 1 - \frac{\sum_{i=1}^{n}(\hat{y}_i - y_i)^2}{\sum_{i=1}^{n}(y_i - \bar{y}_i)^2} \qquad (1)$$

where R^2 is coefficient of determination, *RSS* is coefficient of determination and *TSS* is total sum of squares.

The other statistical model used for regression is Nash-Sutcliffe efficiency (*NSE*) and it indicates how well the plot of observed (*OBS*) versus simulated data (*SIM*) fits the line. NSE is computed as shown in Equation 2:

$$NSE = 1 - \frac{\sum_{i=1}^{n}(OBS_i - SIM_i)^2}{\sum_{i=1}^{n}(OBS_i - \overline{OBS})^2} \qquad (2)$$

Based on the value of *NSE*, the property of the model performance is rated, quantitatively, with four ranks in order of strength, as shown in Table 1.

Table 1: NSE value index from the higher "very good" to the lower "unsatisfactory" rate of correlation strength.

Tablica 1. Vrijednosti NSE indeksa od više „vrlo dobre” do niže „nezadovoljavajuće” stope jakosti korelacije.

Properties	Value
Very good	$0.75 < NSE_h \le 1.00$
Good	$0.65 < NSE_h \le 0.75$
Satisfactory	$0.50 < NSE_h \le 0.65$
Unsatisfactory	$NSE_h \le 0.50$

NSE shows how closely the line fits the plot of real versus simulated values. Higher R^2 and NSE values and lower RMSE values are recommended for evaluation purposes (Behera et al., 2016).

3. RESULTS AND DISCUSSION

3.1. Model calibration and validation

To simulate future climate variables, such as rainfall, the statistical downscaling model (SDSM) was calibrated and validated. Daily precipitation amount is used to downscale the current (1983–2016) and future scenarios (2011–2100) under three representative concentration pathways (RCP2.6, RCP4.5, and RCP8.5). Calibration was done from 1983 to 2000, and validation was from 2001 to 2016. Before generating climate change scenarios, calibration and validation are essential processes in adjusting climate data simulation with the SDSM model, which is used in this study. So, to compare and relate the strength of the model to simulate observed historical data, different correlation approaches are analysed and manipulated by regression models (such as R^2 and Nash-Sutcliffe model efficiency coefficient/NSE). coefficient of determination (R^2) tells us how well the regression model fits the observed data while NSE regression model tells the model efficiency evaluation in simulating the data. In each case, a positive value close to 1 indicates good relation and high model efficiency in simulating the data by the model during calibration and validation. In general, a value greater than 0.5 is considered good.

In the case of the Upper Awash River Basin, the result of model calibration shows high values of R^2 (≥ 0.73, 0.97, 0.91) for precipitation amount in Alem Tena, Guder and Holeta, respectively (Tab. 2). The NSE model evaluation is similar (≥ 0.70, 0.93, 0.86). During the model performance evaluation, the relationship between observed and simulated precipitation data is comparatively strong in Guder, Holeta, and Alem Tena stations, respectively with corresponding R^2 and NSE values.
In general, during the validation period, the study found a good correlation between the modelled data and observed climate records.

In the case of Middle Awash River Basin, during calibration the mean precipitation amount observed and simulated data for three sample stations R^2 and Nash models range between 0.6 (Shewa Robit station) up to 0.79 (Awash Arba station). The value of calibration and validation were greater than 0.5. So, the results of calibration and validation of mean precipitation amount are considered as good. A relatively strong relation in model validation process is observed on Awash Arba station comparatively, with R^2 of 0.79 and NSE of 0.64.

Model performance evaluation in the Lower Awash River Basin is shown in the last three columns in Table 2. The model demonstrated a relatively strong capability in replicating data during the calibration period at the Chefa climate station. For the whole Lower Awash River Basin (average for three representative stations) model was able to replicate the observed precipitation data moderately, with $R^2 = 0.52$ and NSE = 0.5.
Consistent with findings from previous studies (Molla, 2020; Feyissa, Zeleke, Bewket and Gebremariam, 2018), this is likely due to the high variability inherent to precipitation patterns. Current climate models struggle to fully capture the spatial and temporal variability of precipitation, which affects replication accuracy.

Table 2. Model performance evaluation in calibration and validation over Awash River Basin.

Tablica 2. Evaluacija izvedbe modela tijekom kalibracije i validacije na slivu rijeke Awash.

River sub basins		Upper Awash Basin			Middle Awash Basin			Lower Awash Basin		
Stations		Alem Tena	Guder	Holeta	Awash Arba	Shewa Robit	Erer	Chefa	Mille	Dire Dawa
R^2	Calibration	0.73	0.97	0.91	0.68	0.75	0.74	0.70	0.51	0.55
	Validation	0.80	0.97	0.91	0.79	0.70	0.73	0.65	0.42	0.50
NSE	Calibration	0.70	0.93	0.86	0.67	0.67	0.72	0.70	0.44	0.50
	Validation	0.75	0.94	0.86	0.64	0.60	0.72	0.66	0.41	0.41

3.2. Projected future climate change scenario in precipitation amount

3.2.1. Upper Awash River Basin

Three RCPs, which cover a wide range of scenarios, are used to project future precipitation amount and these results are compared to the base period of 1983–2016. The analysis is based on the WMO time frame stated as the 2020s (2011–2040), 2050s (2041–2070), and 2080s (2071–2100).

Figures 3, 4 and 5 show mean annual, seasonal and monthly precipitation amount changes under RCP 2.6, 4.5 and 8.5 emission scenarios for Upper Awash River Basin. Change in mean precipitation amount is the average of changes from three stations in Upper Awash River Basin.

As shown in Figure 3, a result of the analysis based on projection of climate change in RCP2.6 compared to the baseline period exhibited a decrease of rainfall amount in August, September and October. A rainfall projection for Bega (October–January/ONDJ) shows a minor decrease in the 2020s and 2080s, but a slight increase in the 2050s. In above mentioned months the maximum decrease of approximately 28% from the mean is exhibited in the 2080s in October. Belg's season (February–May/FMAM) projection under RCP2.6 emission scenario shows an increase in the 2020s, 2050s, and 2080s by approximately 20%, 32% and 32%, respectively. The Kiremt (June–September/JJAS) season shows no significant change in the 2020s, a slight increase of 1% in the 2050s and a minor decrease of 1% in the 2080s. The annual change in precipitation amount from the mean under RCP2.6 is anticipated to increase by approximately 4% in the 2050s and 2080s, but the change is negligible in the 2020s.

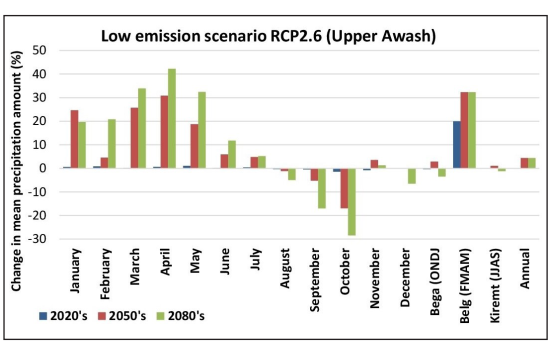

Figure 3. Change in monthly, seasonal, and annual mean precipitation amount under RCP2.6 (Upper Awash River Basin).

Slika 3. Promjena srednje mjesečne, sezonske i godišnje količine oborine za RCP2,6 (gornji sliv rijeke Awash).

For medium emission scenario (RCP4.5), as shown in Figure 4, the monthly mean rainfall start to decrease in August in the 2080s. Higher decrease from the mean is expected in September and October in the 2020s, 2050s, and 2080s. Similarly, a slight decrease is anticipated in November in the 2050s. Looking seasonally, under medium emission scenario (RCP4.5) rainfall in Bega is expected to slightly increase in the 2050s and 2080s (by 2% and 5%), similar as in Kiremt (by 2%, 4%, and 4% in the 2020s, 2050s, and 2080s, respectively). In Belg season (Fabruary–May) the increase is much higher (approximatelly 20%, 20% and 39% in the 2020s, 2050s, and 2080s respectively). The annual change in precipitation amount under RCP4.5 is anticipated to increase by approximately 7% and 10% in the 2050s and 2080s, but insignificant in the 2020s.

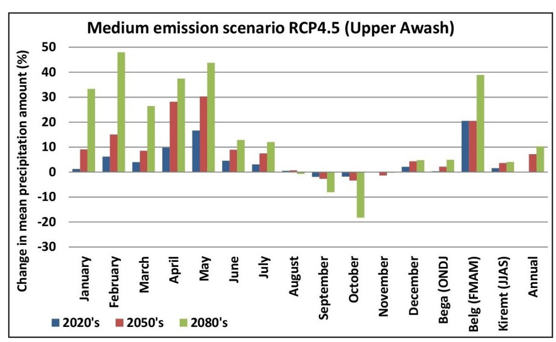

Figure 4. Change in monthly, seasonal, and annual mean precipitation amount under RCP4.5 (Upper Awash River Basin).

Slika 4. Promjena srednje mjesečne, sezonske i godišnje količine oborine za RCP4,5 (gornji sliv rijeke Awash).

Based on Figure 5, the high emission scenario also shows a minor decrease in September in the 2020s and 2050s, but increase in the 2080s. In addition, a minor to moderate decrease is expected in October by approximately 2% in the 2020s, 8% in the 2050s and 5% in the 2080s. Although, there will be increment of rainfall for the rest of the months with the highest value in February by approximately 1%, 28% and 87% in the 2020s, 2050, 2080s, respectively. In the high emission scenario (RCP8.5) rainfall in Bega is expected to slightly increase in the 2020s, 2050s and 2080s. Belg's season projection shows an increase under RCP8.5 emission scenario in the 2020s, 2050s, and 2080s by approximately 1%, 22% and 59%, respectively. In the high emission scenario, the Kiremt season rainfall is expected to increase in the 2050s and 2080s by approximately 5% and 14%, respectively, compared to the baseline mean but there will not be significant change in rainfall in the 2020s. The annual change in precipitation amount is anticipated to increase by approximately 8% and 22% in the 2050s and 2080s, but the change is negligible in the 2020s.

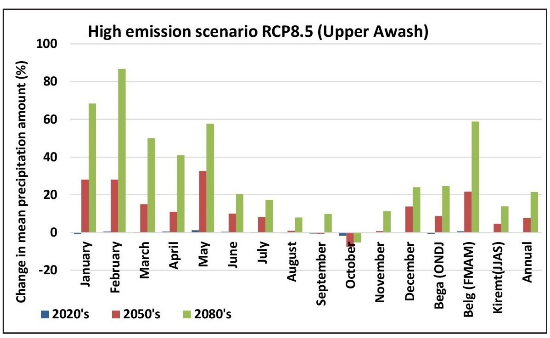

Figure 5. Change in monthly, seasonal, and annual mean precipitation amount under RCP8.5 (Upper Awash River Basin).

Slika 5. Promjena srednje mjesečne, sezonske i godišnje količine oborine za RCP8,5 (gornji sliv rijeke Awash).

In the Upper Awash River sub-basin, except some months mentioned above all the remaining months, seasons and annual condition of precipitation amount exhibited an increase for all time frames (2020s, 2050s and 2080s). In addition, projection for the Belg season (February–May: FMAM) shows an increasing trend for all emission scenarios (RCP 2.6, 4.5, and 8.5) in the 2020s, 2050s, and 2080s. When compared season to season the highest change in precipitation amount is expected to be in Belg season in the 2080s by about 32%, 39% and 59% under the RCP2.6, RCP4.5 and RCP8.5 emission scenario, respectively. The change of mean annual precipitation will be higher in medium and high emission scenarios in the 2080s.

3.2.2. Middle Awash River Basin

Under RCP2.6 scenario, as shown in Figure 6, the monthly mean rainfall decreases in July, August, September, October, December, January and February for all time frames. The maximum decrease is expected in September by 4%, 21% and 40% in the 2020s, 2050s and 2080s, respectively. In November and March a slight decrease from the mean in the 2020s, but an increase in the 2050s and 2080s is shown. Significant increase is anticipated for the rest of the months especially in the 2050s and 2080s. The maximum increase of 10%, 20%, and 33% in the 2020s, 2050s, and 2080s, respectively is expected in April. The rainfall in Bega is expected to decrease in the 2020s, 2050s and 2080s by approximately 4%, 13% and 11%, respectively. Similarly, decrease of rainfall amount is expected in Kiremt season by approximately 1%, 13%, and 9% in the 2020s, 2050s, and 2080s, respectively. On the contrary, Belg's season projection shows an increase by approximately 2%, 15% and 22%, respectively in the 2020s, 2050s, and 2080s. The annual change in precipitation amount under RCP2.6 is anticipated to decrease from the mean by approximately 1%, 2% and 3% in the 2020s, 2050s and 2080s, respectively.

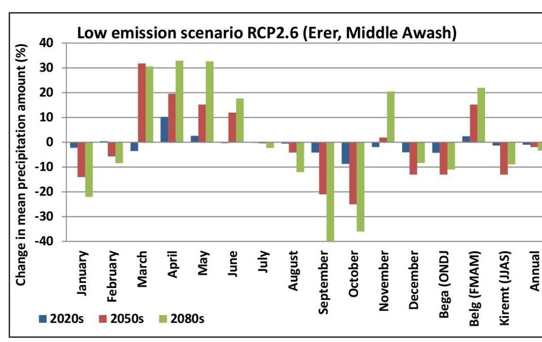

Figure 6. Projected changes in mean monthly, seasonal and annual precipitation amount in the 2020s, 2050s, and 2080s under RCP2.6 for Erer station (Middle Awash River Basin).

Slika 6. Projicirane promjene srednje mjesečne, sezonske i godišnje količine oborine u 2020-ima, 2050-ima i 2080-ima za RCP2,6 za postaju Erer (srednji sliv rijeke Awash).

As shown in Figure 7, under RCP4.5 scenario, the monthly mean rainfall decreases in August, September, October, January and February for all time frames. The maximum decrease is expected in January by 6%, 20% and 30% in the 2020s, 2050s and 2080s respectively. On the other hand, a significant increase is anticipated for the rest of the months especially in the 2050s and 2080s. The maximum increase is expected in May by approximately 7%, 50%, and 66% in the 2020s, 2050s, and 2080s, respectively. The Bega rainfall is expected to decrease slightly approximately by 2% in 2020s; and negligible in 2050s and 2080s. Belg's season projection shows an increase in the 2020s, 2050s, and 2080s by around 4%, 20% and 36%, respectively. While, the Kiremt season rainfall is expected to have almost negligible change in all time frames. The annual change in precipitation amount from the mean under RCP4.5 is anticipated to increase by approximately 5% and 7% in the 2050s and 2080s, but negligible in the 2020s.

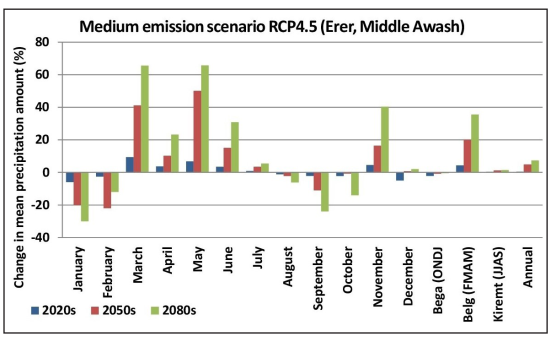

Figure 7. Projected changes in mean monthly, seasonal and annual precipitation amount in the 2020s, 2050s, and 2080s under RCP4.5 for Erer station (Middle Awash River Basin).

Slika 7. Projicirane promjene srednje mjesečne, sezonske i godišnje količine oborine u 2020-ima, 2050-ima i 2080-ima za RCP4,5 za postaju Erer (srednji sliv rijeke Awash).

As shown in Figure 8, under RCP8.5 scenario, the monthly mean rainfall decreases in the period from August till February, especially in the 2050s and 2080s. The maximum decrease by 26% is expected in October in the 2050s and in January by 24% in the 2080s. In the 2020s decrease is the highest in February (by less than 10%) and negligible in other months. On the other hand, a significant increase is anticipated in March, April, May and June, especially in the 2050s and 2080s. The maximum increase by approximately 7%, 48%, and 79% in the 2020s, 2050s, and 2080s, respectively is expected in May. The Bega rainfall is expected to decrease by approximately 18% and 15% in 2050s and 2080s, but a slight increase by approximately 2% in the 2020s. Belg's season projection shows an increase in the 2050s and 2080s by around 15% and +50%, respectively, but a slight decrease by 2% in 2020s. While, the Kiremit season rainfall is expected to increase by about 1%, 2% and 5% in the 2020s, 2050s, and 2080s, respectively. The annual change in precipitation amount from the mean, under RCP8.5, is anticipated to increase by approximately 9% in 2080s, but almost negligible change is expected in the 2020s and 2050s.

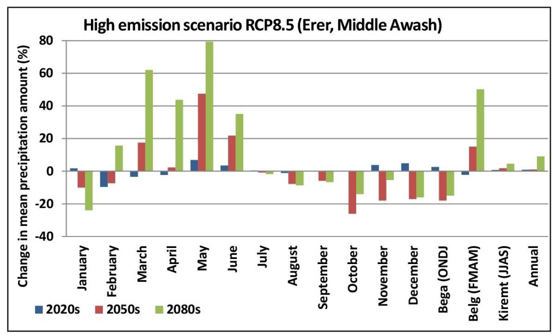

Figure 8. Projected changes in mean monthly, seasonal and annual precipitation amount in the 2020s, 2050s, and 2080s under RCP8.5 for Erer station (Middle Awash River Basin).

Slika 8. Projicirane promjene srednje mjesečne, sezonske i godišnje količine oborine u 2020-ima, 2050-ima i 2080-ima za RCP8,5 za postaju Erer (srednji sliv rijeke Awash).

Under Middle Awash sub-river catchment the results showed the highest increase in mean rainfall in the Belg season, under RCP2.6, RCP4.5 and RCP8.5, almost in all time frames (2020s, 2050s and 2080s). The highest increment in 2080s is approximately 22%, 36% and 50% in the Belg season, under RCP2.6, RCP4.5 and RCP8.5, respectively. In other words, compared to other seasons, the Belg season showed significant increment change from the base line period almost for all time frames and all scenarios.

3.2.3. Lower Awash River Basin

Figures 9, 10 and 11 demonstrate the future precipitation amount projection change from base line period based on RCP2.6, RCP4.5 and RCP8.5 emission scenarios for all time frames for Lower Awash River Basin represented by Dire Dawa station.

Under RCP2.6 scenario, as shown in Figure 9, the monthly mean rainfall slightly decreases in October, November, December, March and June in the 2020s; but moderately increases in the 2050s and 2080s on the aforementioned months. The maximum decrease is expected in October and November by approximately 3% in the 2020s. The maximum increase is expected in December with 28% and 17% in the 2050s, and 2080s, respectively. The Bega rainfall is expected to slightly decrease in the 2020s; but increase in the 2050s and 2080s approximately by 17% and 9%, respectively. Belg's season projection shows an increase for the 2020s, 2050s, and 2080s approximately by 2%, 16% and 6%, respectively. Similarly, the Kiremt season rainfall is expected to increase approximately by 2%, and 3% in the 2050s and 2080s, but almost nothing in the 2020s. The annual change in precipitation amount from the mean, under RCP2.6, is anticipated to increase by approximately 1%, 6% and 4% in the 2020s, 2050s and 2080s, respectively.

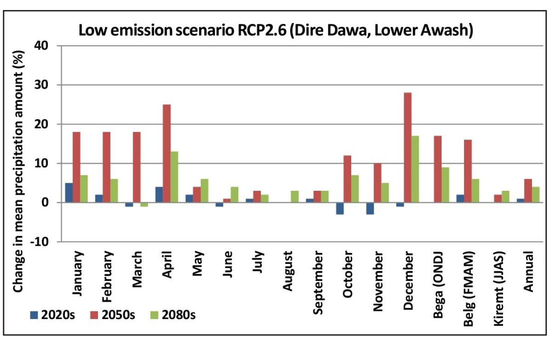

Figure 9. Projected changes in mean monthly, seasonal and annual precipitation amount in the 2020s, 2050s, and 2080s under RCP2.6 for Dire Dawa station (Lower Awash River Basin).

Slika 9. Projicirane promjene srednje mjesečne, sezonske i godišnje količine oborine u 2020-ima, 2050-ima i 2080-ima za RCP2,6 za postaju Dire Dawa (donji sliv rijeke Awash).

As shown in Figure 10, under RCP4.5 scenario, the monthly mean rainfall slightly decreases in March and April only in the 2020s, compared to historical mean (baseline). On the other hand, a significant increase is anticipated for the rest of the months especially in the 2050s and 2080s. The maximum increase is in January with approximately 3%, 17%, and 39% and in December with approximately 5%, 22%, and 36% in the 2020s, 2050s, and 2080s, respectively. The Bega rainfall is expected to increase approximately by 3%, 19% and 34% in the 2020s, 2050s and 2080s, respectively. Belg's season projection shows an increase in the 2050s and 2080s by approximately 12% and 26%, but almost negligible in the 2020s. While, the Kiremt season rainfall is expected to increase minimal in 2020s; and significant in the 2050s and 2080s by approximately 11% and 19%, respectively. The annual change in precipitation amount from the mean, under RCP4.5 is anticipated to increase by approximately 1%, 12% and 23% in the 2020s, 2050s and 2080s, respectively.

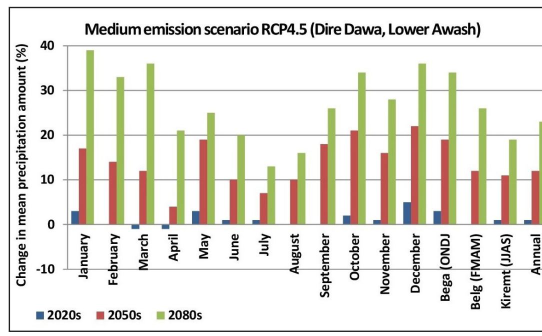

Figure 10. Projected changes in mean monthly, seasonal and annual precipitation amount in the 2020s, 2050s, and 2080s under RCP4.5 for Dire Dawa station (Lower Awash River Basin).

Slika 10. Projicirane promjene srednje mjesečne, sezonske i godišnje količine oborine u 2020-ima, 2050-ima i 2080-ima za RCP4,5 za postaju Dire Dawa (donji sliv rijeke Awash).

As shown in Figure 11, under RCP8.5 scenario the monthly mean rainfall slightly decrease in February, March and April only in 2020s. Though, a significant increase is expected for the rest of the months especially for 2050s and 2080s. The maximum increase is in October with approximately 9%, 22%, and 80% and December with approximately 6%, 48%, and 71% in the 2020s, 2050s, and 2080s, respectively. The Bega rainfall is expected to increase approximately by 4%, 22% and 59% in 2020s, 2050s and 2080s, respectively. Belg's season projection shows an increase in the 2050s and 2080s approximately by 12% and 36%, respectively, but a slight decrease by approximately 3% in 2020s. While, the Kiremt season rainfall is expected to increase by about 2%, 9% and 21% in the 2020s, 2050s, and 2080s, respectively. The annual change in precipitation from the mean, under RCP8.5, is anticipated to increase approximately by 1%, 11% and 27% in the 2020s, 2050s and 2080s, respectively.

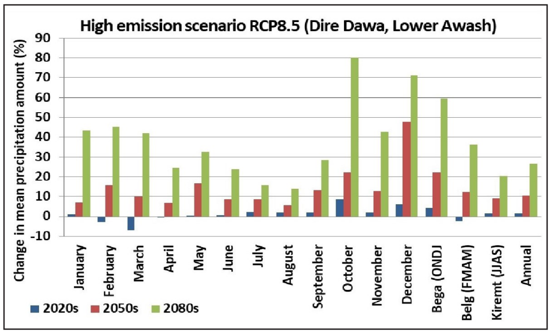

Figure 11. Projected changes in mean monthly, seasonal and annual precipitation amount in the 2020s, 2050s, and 2080s under RCP8.5 for Dire Dawa station (Lower Awash River Basin).

Slika 11. Projicirane promjene srednje mjesečne, sezonske i godišnje količine oborine u 2020-ima, 2050-ima i 2080-ima za RCP8,5 za postaju Dire Dawa (donji sliv rijeke Awash).

For Lower Awash River Basin, the model output showed the highest change in mean precipitation amount in Bega season compared to the other seasons, under all RCPs and time frames. The highest increment in the Bega season in the 2080s is approximately 9%, 34% and 59%, under RCP2.6, RCP4.5 and RCP8.5, respectively.

4. CONCLUSIONS AND RECOMMENDATIONS

Regarding model calibration and validation evaluation, the model was very good in replicating the observed precipitation amount data over most of the climate stations, but over a few stations the calibration and validation process were moderate. This is due to high variability and uncertainty associated with the nature of precipitation and the current climate models could not fully capture spatial and temporal variability of precipitation amount. This fact is also similar with the research study done by Molla (2020) and other related studies.

Regarding projection of future climate scenarios, the precipitation amount exhibited an increase ranging from 1% up to 87% (Upper Awash, RCP8.5 in the 2080s in February), but in some months a decrease is observed ranging from 1% up to 40% (Middle Awash, RCP2.6 in the 2080s in September), compared to the baseline period (1983–2016). When compared season to season, over Upper and Middle Awash River Basin, the highest change in precipitation amount increment is expected to be in the Belg season; while in the Bega season over Lower Awash River Basin. When we consider the future annual precipitation amount outlook, the Lower Awash River Basin is expected to experience the highest increase changes in precipitation amount compared to the Middle and Upper Awash River Basins.

In general, we conclude that the future climate changes will significantly increase precipitation amount from time to time over the Awash River Basins. As a result, the river basin will be vulnerable to flooding due to the anticipated increase in precipitation amount brought on by global climate change; and are likely to have moderate to significant negative impacts on various socioeconomic activities over the communities and natural resources existing over Awash River Basin.

In order to create better climate change adaptation and mitigation mechanisms, it is advised that decision-makers should be aware of this data and other related findings and strengthen the national adaptation and mitigation strategies. Hence, early warning programs and response strategies should be implemented to support and strengthen soil management and forest rehabilitation activities to minimize environmental impacts like degradation and reservoir sedimentation and flood impacts. Further studies also need to be undertaken by adding different model ensembles in order to avoid prediction inconsistency, which will be informative and supportive for further investigations.

REFERENCES

Abayneh, T.G., G. Ephrem and D. Hayal, 2024: GIS and Remote sensing-based land use land cover change classification map, interlinked with population growth dynamics in Awash River Basin (ARB), Ethiopia. https://doi.org/10.21203/rs.3.rs-4528962/v1.

Arora, V.K. and G.J. Boer, 2014: Terrestrial ecosystems response to future changes in climate and atmospheric CO_2 concentration. *Biogeosciences Discuss*., **11**, 3581–3614, www.biogeosciences-discuss.net/11/3581/2014/, https://doi.org/10.5194/bgd-11-3581-2014.

Behera, S. et al., 2016: Application of Statistical Downscaling Model for Prediction of Future Rainfall in Bhudhabalanga River Basin, Odisha (India). *IJEAT*, **5**(4), 24–30.

Berhanu, W. and F. Beyene, 2015: Climate Variability and Household Adaptation Strategies in Southern Ethiopia. *Sustainability*, **7**(6), 6353–6375, https://doi.org/10.3390/su7066353.

Degefu, W., 1987: Some aspects of meteorological drought in Ethiopia. 223–236, in Glantz, M.H. (Ed.), *Drought and Hunger in Africa: Denying Famine a Future*, Cambridge University Press, 457 pp.

Dibike, Y.B. and P. Coulibaly, 2005: Hydrologic impact of climate change in Saguenay watershed: comparison of downscaling methods and hydrologic models. *J. Hydrol.,* **307**(1-4), 145–163, https://doi.org/10.1016/j.jhydrol.2004.10.012.

Dirmeyer, P.A., Y. Jin, B. Singh and X. Yan, 2013: Evolving land–atmosphere interactions over North America from CMIP5 simulations. *J. Clim.*, **26**(19), 7313–7327, https://doi.org/10.1175/JCLI-D-12-00454.1.

Eden, J.M. and M. Widmann, 2014: Downscaling of GCM-Simulated Precipitation Using Model Output Statistics. *J. Clim.*, **27**(1), 312–324, https://doi.org/10.1175/JCLI-D-13-00063.1.

Fan, X., L. Jiang and J. Gou, 2021: Statistical downscaling and projection of future temperatures across the Loess Plateau, China. *Weather Clim. Extrem.*, **32**, https://doi.org/10.1016/j.wace.2021.100328.

Fenglin, W. et al., 2023: Exploratory regression modelling for flood susceptibility mapping in the GIS environment. *Sci. Rep.*, **13**(247), https://doi.org/10.1038/s41598-023-27447-0.

Feyissa, G., G. Zeleke, W. Bewket and E. Gebremariam, 2018: Downscaling of Future Temperature and Precipitation Extremes in Addis Ababa under Climate Change. *Climate*, **6**(3), https://doi.org/10.3390/cli6030058.

Fowler, H.J., S. Blenkinsop and C. Tebaldi, 2007: Linking climate change modelling to impacts studies: recent advances in downscaling techniques for hydrological modelling. *Int. J. Climatol.*, **27**(12), 1547–1578.

Frich, P. et al., 2002: Observed coherent changes in climatic extremes during the second half of the twentieth century. *Clim. Res.*, **19**, 193–212.

Gebrechorkos, S.H., S. Huelsmann and C. Bernhofer, 2018: Changes in temperature and precipitation extremes in Ethiopia. *Int. J. Climatol.*, **39**, 18–30, https://doi.org/10.1002/joc.5777.

Gebrechorkos, S.H., S. Huelsmann and C. Bernhofer, 2019: Statistically downscaled climate dataset for East Africa. *Scientific Data*, **6**(31), https://doi.org/10.1038/s41597-019-0038-1.

Gilgel, A.W., T. Terefe and M. Asfaw, 2019: Assessment and Projection of Climate Change Impacts on Malaria Distribution in Ethiopia: Case of Combolcha and Debark Districts. *IJRES*, **5**(4), 20–42, http://dx.doi.org/10.20431/2454-9444.0504003.

Giorgetta, M.A. et al., 2013: Climate and carbon cycle changes from 1850 to 2100 in MPI-ESM simulations for the Coupled Model Intercomparison Project phase 5. *J. Adv. Model. Earth Syst.*, **5**(3), 572–597, https://doi.org/10.1002/jame.20038.

Haile, G.G. et al., 2020: Long-term spatiotemporal variation of drought patterns over the Greater Horn of Africa. *Sci. Total Environ.*, **704**, https://doi.org/10.1016/j.scitotenv.2019.135299.

Hassan, Z., S. Shamsudin and S. Harun, 2013: Application of SDSM and LARS-WG for simulating and downscaling of rainfall and temperature. *Theoretical and Applied Climatology*, **116**, 243–257, https://doi.org/10.1007/s00704-013-0951-8.

Houghton, J.T. et al., 2001: Climate change 2001: The Scientific Basis. Contribution of Working Group I to the Third Assessment Report of the Intergovernmental Panel on Climate Change, Cambridge University Press.

Huang, J. et al., 2010: Estimation of future precipitation change in the Yangtze River basin by using statistical downscaling method. *SERRA*, **25**, 781–792; https://doi.org/10.1007/s00477-010-0441-9.

Hui, Y. et al, 2019: Bias nonstationarity of global climate model outputs: the role of internal climate variability and climate model sensitivity. *Int. J. Climatol.*, **39**(4), https://doi.org/10.1002/joc.5950.

Hutchinson, M.F. et al., 2009: Development and testing of Canada-wide interpolated spatial models of daily minimum–maximum temperature and precipitation for 1961–2003. *J. Appl. Meteor. Climatol.*, **48**(4), 725–741, https://doi.org/10.1175/2008JAMC1979.1.

IPCC, 2014: Climate Change 2014: Synthesis Report. Contribution of Working Groups I, II and III to the Fifth Assessment Report of the Intergovernmental Panel on Climate Change.

IPCC, 2021: Climate Change 2021: The Physical Science Basis. Contribution of Working Group I to the Sixth Assessment Report of the Intergovernmental Panel on Climate Change. https://doi.org/10.1017/9781009157896.

Koriche, S. A, T. Rientjes, A.T. Haile and S. Bekele, 2012: Remote Sensing Based Hydrological Modelling for Flood Early Warning in the Upper and Middle Awash River Basin, https://doi.org/10.13140/RG.2.1.4882.6487.

Lee, C-Y., S. Camargo, A.H. Sobel and M.K. Tippet, 2020: Statistical-Dynamical Downscaling Projections of Tropical Cyclone Activity in a Warming Climate: Two Diverging Genesis Scenarios. *J. Clim.*, **33**(11), 4815–4834, https://doi.org/10.1175/JCLI-D-19-0452.1.

Liu, J., C.D. Kummerow and G.S. Elsaesser, 2017: Identifying and analysing uncertainty structures in the TRMM Microwave Imager precipitation product. *Int. J. Remote Sens.*, **38**(1), 23–42, https://doi.org/10.1080/01431161.2016.1259676.

McCarthy, J.J. et al., 2001: Climate change 2001: Impacts, Adaptation, and Vulnerability. Contribution of Working Group II to the Third Assessment Report of the Intergovernmental Panel on Climate Change. Cambridge Univ. Press, Cambridge, UK.

Mishra, V. et al., 2014: Reliability of regional and global climate models to simulate precipitation extremes over India. *J. Geophys. Res. Atmos.*, **119**(15), 9301–9323, https://doi.org/10.1002/2014JD021636.

Molla, M., 2016: Climate Variability, its impact on Maize Production and Adaptation options: Case Study of Halaba Special Woreda, Southern Ethiopia. https://doi.org/10.13140/RG.2.2.19426.27843.

Molla, M., 2016a: Prediction of Future climate and its Impact on Crop Production and possible adaptation Strategy. SNNPR Shashogo woreda, Ethiopian Environments and Forest Research Institute Hawassa Center, Ethiopia.

Molla, M., 2020: Statically Downscaling using different Representative Concentration Pass ways of Emission Scenario; in the Case Wolikite, Southwest Ethiopia. *Int. J. Environ. Sci. Nat. Res.*, **25**(3), https://doi.org/10.19080/IJESNR.2020.25.556162.

Molla, M., 2020a: Developing Climate Change Projections using Different Representative Concentration Pathways of Emission Scenario In the Case Jimma, Ethiopia. *Int. J. Environ. Sci. Nat. Res.,* **25**(4), 199–209, https://doi.org/10.19080/IJESNR.2020.26.556175.

Nakicenovic, N. and R. Swart, 2000: Special Report on Emissions Scenarios. A special report of Working Group III of the Intergovernmental Panel on Climate Change. Cambridge University Press, Cambridge, 599 pp.

NAPA-ETH, 2019: Climate Resilient Green Economy (CRGE). Ethiopia National Adaptation Plan (NAP-ETH), climate change in the country development policy framework.

Poitras, V. et al., 2011: Projected changes to stream flow characteristics over Western Canada as simulated by the Canadian RCM. *J. Hydrometeorology*, **12**(6), 1395–1413, https://doi.org/10.1175/JHM-D-10-05002.1.

Ranasinghe, R. et al., 2021: Chapter 12: Climate change information for regional impact and for risk assessment. In *Climate Change 2021: The Physical Science Basis*. Contribution of Working Group I to the Sixth Assessment Report of the Intergovernmental Panel on Climate Change, Cambridge University Press, 1767–1926, https://doi.org/10.1017/9781009157896.014.

Romilly, T.G. and M. Gebremichael, 2010: Evaluation of satellite rainfall estimates over Ethiopian river basins. *Hydrol. Earth Syst. Sci.*, **15**, 1505–1514, https://doi.org/10.5194/hess-15-1505-2011.

Separovic, L. et al., 2013: Present climate and climate change over North America as simulated by the fifth-generation Canadian regional climate model. *Clim. Dyn.*, **41**, 3167–3201, https://doi.org/10.1007/s00382-013-1737-5.

Tavakol-Davani, H., M. Nasseri and B. Zahraie, 2013: Improved statistical downscaling of daily precipitation using SDSM platform and data-mining methods. *Int. J. Clim.*, https://doi.org/10.1002/joc.3611.

Van Vuuren, D.P. et al., 2011: The representative concentration pathways: an overview. *Clim. Change*, **109**(5), https://doi.org/10.1007/s10584-011-0148-z.

Wilby, R.L., et al. 2000: Hydrological responses to dynamically and statistically downscaled climate model output. *Geophys. Res. Lett.*, **27**(8), 1199–1202, https://doi.org/10.1029/1999GL006078.

Wilby, R.L. et al., 2002: SDSM – a decision support tool for the assessment of regional climate change impacts. *Environ. Model. Softw.*, **17**(2), 145–157, https://doi.org/10.1016/S1364-8152(01)00060-3.

Wilby, R.L. and C.W. Dawson, 2007: Using SDSM Version 3.1 – A decision support tool for the assessment of regional climate change impacts – User Manual, https://www.researchgate.net/publication/266456667.

Wilby, R.L. et al., 2014: The Statistical DownScaling Model – Decision Centric (SDSM-DC): conceptual basis and applications. *Clim. Res.,* **61**, 259–276, https://doi.org/10.3354/cr01254.

Yang, D. et al., 2020: Integrating the InVEST and SDSM Model for Estimating Water Provision Services in Response to Future Climate Change in Monsoon Basins of South China. *Water*, **12**(11), 1–16, https://doi.org/10.3390/w12113199.

Zhao, F.F., Z.X. Xu, J.X. Huang and J.Y. Li, 2008: Monotonic trend and abrupt changes for major climate variables in the headwater catchment of the Yellow River basin. *Hydrological Processes*, **22**(23), 4587–4599, https://doi.org/10.1002/hyp.7063